Towards multifunctional geoengineering material for eutrophication remediation: simultaneously control internal nutrient (N&P) load and tackle hypoxia

ABSTRACT

An effective approach for control of internal nutrient loading and sediment hypoxia remains a longstanding challenge to the restoration of aquatic ecosystems. In order to simultaneously tackle these issues, a MultiFunction Geoengineering material (MFG) was developed for sediment remediation through the synergistic functions of physical capping, nutrient adsorption and delivery of O_2 nanobubbles. The MFG, derived from natural zeolite, exhibited superior (1.5-4 times higher) adsorption capabilities of both phosphate (P) and ammonium (N) than pristine zeolite. The O_2 adsorption capacity was also enhanced from 46 to 121 mg O_2/g for the MFG. An in-situ sediment capping experiment in a eutrophic lake demonstrated that the application of MFG dramatically reversed sediment hypoxia (ORP -200 mV) to an aerobic status (ORP 175 mV) and stimulated sediment microbial activity, particularly nitrifying bacteria. The comprehensive functionalities of the material were for the first time quantified, where O_2 nanobubble delivery was determined to be the largest contributor to changing the sediment from a nutrient source to a sink through decreasing 206% and 156% of the P and N fluxes from the sediment, respectively. Our findings highlight the viability of such multifunctional material for the remediation of internal nutrient loads, towards sustainable eutrophication control.

Keywords: Eutrophication, internal nutrient loading, lake or river restoration, oxygen nanobubble, sediment remediation

1. Introduction

Eutrophication of water bodies, both natural and artificial, is spreading worldwide, causing serious consequences such as Harmful Algal Blooms (HABs)[1] and/or black odorous water[2]. These nuisance phenomena pose serious threats to the aquatic ecosystem, environment, and to public health[3]. It is agreed that management of the dual nutrients, nitrogen (N) and phosphorus (P), could produce a sustainable, long-term, improvement in lake water quality towards remediation of eutrophication[4]. However, consequent to the control of external nutrient loading from anthropogenic discharges through strict statutory requirements and implementations, internal loadings of N and P from sediments can be expected to further increase the occurrence of HABs and deliver continuous pressure on aquatic ecosystems over the subsequent decades[5, 6]. Therefore, measures for reduction of internal loadings to eliminate nutrient N and P, have recently attracted increasing attention.

Various approaches have been developed to reduce the nutrient loadings from sediment, including dredging[7], oxygenation[8], use of chemical flocculants[9] and *in situ* capping[10]. Among them, capping of contaminated sediment has been suggested to be potentially the most effective method for the control of eutrophication in lakes[11, 12]. Capping treatment by the spraying of natural materials, such as sand, clay, gravel and rock, in lakes could form a physical barrier on surficial sediments and effectively prevent nutrients from entering into the water. Synthetic materials, such as lanthanum-modified bentonite (Phoslock™) and aluminium-modified zeolite (Aqual-P), have been developed to augment the functionality from purely existing as a physical barrier to additionally acting as an active P adsorbed[13, 14]. Moreover, some synthetic materials have also been used to further adsorb both P and N released from sediments[15]. However, such materials mainly focus on improvements in adsorption capacity, while ignoring the fact that the adsorbed and capped P and N may subsequently be re-released into overlying water due to the aging of materials and changes in the environmental conditions, such as low redox potential[16].

In eutrophic waters, the consequent oxygen depletion by mineralisation of senescent algal blooms induces hypoxia/anoxia at the sediment-water interface (SWI)[17]. The

hypoxia/anoxia condition can significantly facilitate the mobility of P and N from sediment to waters[18]. Only by reversal of such hypoxia/anoxia at the SWI back to aerobic conditions, can P be firmly adsorbed by the metal oxide-hydroxide complexes[19] and by stimulation of microbial-induced nitrification process ammonium release can be further prevented[20]. Therefore, successful tackle of the hypoxia/anoxia at SWI is crucial towards the sustainable control of the internal nutrient loadings. However, traditional capping treatment can hardly remediate sediment hypoxia owing to the absence of extra oxygen delivery. Hence, an urgent need exists to develop novel geoengineering materials to not only simultaneously adsorb P and N released from the sediment, but also reverse the hypoxic conditions at the SWI.

Traditional SWI oxygenation methods, such as deep water aeration, have been reported to be hindered due to excessive costs, high energy consumption and hydrologic disturbance of the benthos[21]. Interfacial/surficial oxygen nanobubble technology was first developed in 2018, using natural minerals loaded with oxygen, delivering nano-scale oxygen bubbles into sediment surfaces in a cost-effective and environmentally- friendly way[22]. This study has demonstrated that the synergy of diffusion of oxygen nanobubbles and retention of oxygen at the SWI could successfully reverse conditions of hypoxia and reduce the flux of N and P from sediment. These effects have been attributed to the characteristic longevity and high gas solubility of nanobubbles. Following this concept, further studies have been conducted by different researchers, mainly focused on the performance evaluation of hypoxia/anoxia conversion[23], control of nutrient turnover[24], and modulation of organics mineralization[25]. However, the quantitative contribution of oxygen delivery and capping treatment on the control of the internal nutrient loading has not hitherto been investigated.

This study aimed to develop a multifunctional geoengineering material, which could maximise control of internal nutrient loading through physical capping, nutrient adsorption and remediation of hypoxia at the SWI. Natural zeolite, as an effective ammonium adsorbent, was selected as the skeleton material. This was then modified in order to increase its capabilities for P adsorption and oxygen nanobubble delivery. The

material was initially characterised for mineral composition and surface properties. The theoretical abilities for N, P and oxygen adsorption were also determined. Furthermore, an *in-situ* mesocosm experiment was conducted in a eutrophic lake in order to evaluate real-life performance. Moreover, the contributions of the different functionalities, i.e. oxygen delivery, nutrient adsorption and capping treatment, of the material were quantitatively studied. Dynamics of compositional changes in microbial communities in the sediment before and after treatment were compared in order to support the proposed remediation mechanisms.

2. Materials and methods

2.1 Preparation of MultiFunctional Geoengineering (MFG) material

Natural zeolite, which was recognised to have effective ammonium adsorption ability[26], was selected as the raw material for further modification. Prior to use, the commercially-available zeolite mineral (Ø 1-2 mm), purchased from Yongjia Natural Minerals Ltd., Hebei, China, was passed through a 100-mesh sieve and washed three times with deionized water prior to drying at 105°C for 24 hours.

In order to improve its P adsorption ability, the natural zeolite was further modified using NaOH and $AlCl_3$ before granulation. Specifically, the zeolite was immersed into 1M NaOH (solid:liquid=1:6 w/w), stirred for 2h, and then aged for 24h at 25°C. Precipitates were further washed three times with deionized water and then soaked in 1M $AlCl_3$ (solid: liquid=1:6 w/w), stirred again for 2h and then aged for 24h. The resultant solid was then granulated into spherical particles (Ø 3-5 mm) by ball mill (LG-120A, China). After drying in air, the particles were transferred into a furnace and calcined at 800°C (10°C min^{-1} heating rate) under flowing N_2 for 3h. The modified zeolite was then obtained.

To develop the multifunctional material capable of delivering O_2 to combat sediment hypoxia, the O_2 nanobubble modification was effected through Pressure Swing Adsorption[22]. Briefly, the dried modified zeolite was placed into a pressure-resistant and airtight container and held under vacuum (-0.08 to 0.1MPa) for 2h. Then, pure O_2 (99.99%) was pumped into the container and held at a pressure of 0.12 - 0.15 MPa for a further 4 h. This cyclical vacuum and O_2 nanobubble-loading process was repeated three

times in order to achieve O_2 supersaturation in the modified zeolite. Then, the multifunctional geoengineering materials (MFG) were finally obtained.

2.2 Materials characterization

The textural properties including surface areas and pore volumes of both natural and modified zeolites were determined by the Brunauer-Emmett-Teller (BET) method using a Micromeritics ASAP 2020 instrument (Micromeritics, Inc., USA). X-ray photoelectron spectra (XPS; ESCALAB250Xi, ThermoFisher, USA) was used to determine the major components of the two materials. The surface morphologies of the samples were observed by scanning electron microscope (SEM; JSM-6700F, Japan). The surface chemical properties were analysed using Fourier Transform Infrared spectroscopy (FT-IR; Tensor27, Bruker, Germany), scanning the range 4000-400 cm^{-1}. X-ray powder diffraction (XRD) was performed using a X' Pert Pro MPD X-ray Diffractometer (Philips, Netherlands) to determine mineral compositions.

2.3 Evaluation of N&P adsorption

Phosphate adsorption isotherm determinations were conducted in Erlenmeyer flasks (100 ml) by mixing various concentrations of KH_2PO_4 solutions with 0.5 g of natural zeolite or modified zeolite, respectively, with addition of 0.01 mol/L NaCl to maintain ionic strength. The mixtures were then agitated (25°C, 200 rpm, 24 h) allowing the adsorption to reach equilibrium. After 24 h, the suspensions were filtered (0.45 μm) and phosphate concentration determined by the molybdenum-blue ascorbic acid method. Ammonium adsorption isotherms determinations were carried out by using the same procedure, except that NH_4Cl solution was used, instead of KH_2PO_4. Both adsorption experiments were carried out at pH 7.0.

2.4 Oxygen-loading capability determination

The O_2 adsorption capacities of both natural and modified zeolites were determined by Temperature Programmed Desorption (O_2-TPD; Micromeritics Chemisorb 2720 apparatus). During the test, the sample (10 mg) was placed in a quartz micro-reactor and treated with pure O_2 at 600°C for 1h until the material was saturated. It was then cooled to 50°C under flowing O_2, and the gas was switched to helium for 30 min in order to purge

the O_2 gas from the reactor. Subsequently, the O_2 desorption process was carried out at $600°C$ in helium (40 ml min^{-1}; temperature increase $10°C$ min^{-1}). The O_2 signal, detected by thermo conductivity detector, represented the dynamics of O_2 release from the zeolite materials. In order to quantify the amount of oxygen desorbed from the materials, thermogravimetric analysis (TG; Seteram, Labsys) was performed, to determine the mass lost from the materials during the desorption process. Firstly, 10 mg of material was placed in a platinum TGA pan and saturated with O_2 gas. Then, N_2 gas (25 mL/min) was substituted and the material gradually heated to $800°C$ at 10 $°C$/min. A vacuum was then applied to the instrument and maintained for 300 mins. The dynamics of changes in sample mass were recorded.

2.5 Lacustrine In-situ experiment

2.5.1 Experimental operation

An *in-situ* mesocosm experiment was carried out in July and August, in a shallow eutrophic lake, located at Suzhou Street in Beijing, China (39°59'N, 116°16'E; Fig. 1a). The lake has a total surface area of 220 ha, average depth of 1.8 m and suffered annually from eutrophication, especially in the summer months[27]. Eight mesocosm tubes, each with a 20-cm inner diameter and height of 160 cm, were used to insert into the sediment of the lake to form 120 cm deep water columns and 30 cm sediment cores (Fig. 1b). Duplicate control mesocosms, and those containing capping treatments by natural zeolite, modified zeolite and our multifunctional geoengineering material (MFG), were constructed. After 2 days' stabilization period, the different treatment materials (each of *ca*. 100 g) were applied in respective columns, resulting in a 2 cm depth capping layer above the surficial sediment (Fig. 1c). Notably, extra 2 tubes in Fig. 1b were inserted as the control were destroyed maybe by the fishes and fall down during the experiment.
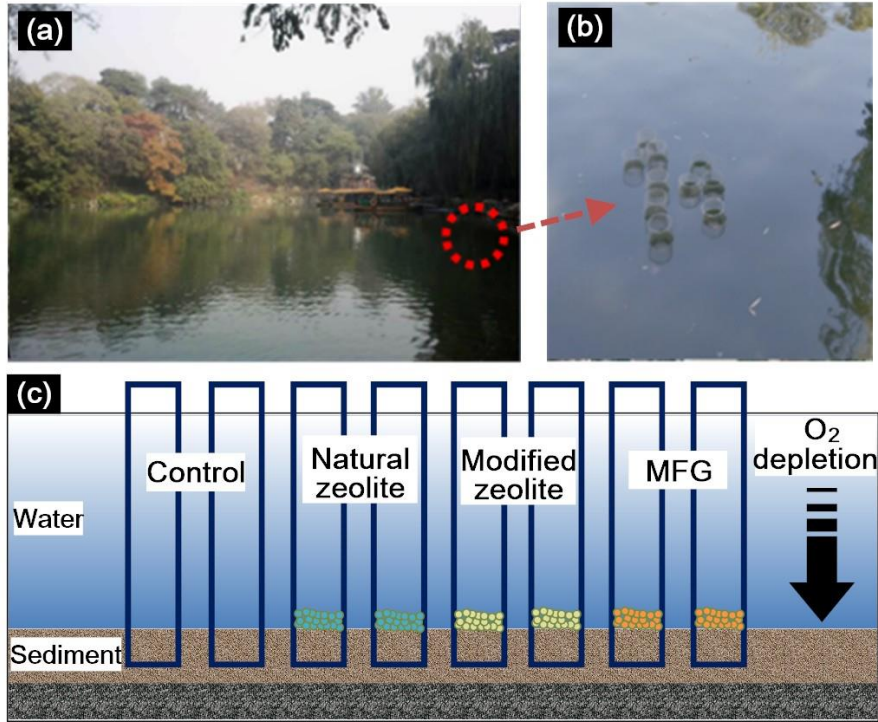
Fig. 1. Location of the *in-situ* experiment in the eutrophic shallow lake (a), general scene (b) and schematic description (c) of the mesocosm columns. MFG (multifunction geoengineering material) represents the O_2 nanobubble loaded modified zeolite.

2.5.2 Water sampling and nutrient quantification

During the experiment, overlying water samples (100 mL) from each column were carefully collected from 5 cm above the sediment using a syringe with a siphon at day 1, 3, 5, 7, 10, 13, 16, 19, 21, 25, 28, 31, and 35. The DO and ORP were measured *in-situ* concurrently with the sampling activities using a Yellow Springs Instruments Proplus (YSI, Ohio, USA). The collected water samples were measured for nutrient concentrations (TP, PO_4^{3-}-P, TN, NH_4^+-N, NO_3^--N, and NO_2^--N). After each sample collection, all columns were slowly replenished with lake water to compensate for the sampling losses.

TP and PO_4^{3-}-P were determined by the potassium persulfate digestion-Mo-Sb-Vc colorimetric method, TN using an alkaline potassium persulphate digestion−ultraviolet spectroscopy method, NH_4^+-N with Nessler's colorimetric method, and NO_3^--N, and NO_2^--N with an ultraviolet colorimetric method[28]. The nutrient fluxes of both N and P were calculated according to the following Equation (1):

$$F_n = \frac{\left[V(C_n - C_0) + \sum_{j-1}^{n} V_{j-1}(C_{j-1} - C_i)\right]}{S \times t} \tag{1}$$

where F_n is the nutrient flux on n^{th} day ($mg\ m^{-2}\ d^{-1}$). C_0 is the nutrient concentration ($mg\ L^{-1}$) before treatment. V and V_j are the volume of overlying water and sampling water (L), respectively. C_n and C_{j-1} are the nutrient concentration ($mg\ L^{-1}$) on n^{th} and j-1th sampling day and before treatment, respectively. C_i is the nutrient concentration of the replenished water ($mg\ L^{-1}$). S is the cross-sectional area of column (m^2) and t is the incubation time (d).

2.5.3 Sediment sampling and microbial community characterisation

In order to study the dynamics of composition of the benthic microbial community, 1.0 g triplicated surface sediment samples (~5cm depth) were taken from each column before and after the experiment, and microbial DNA was extracted using a FastDNA Soil DNA Kit (Omega Bio-tek, USA), based on the manufacturer's recommendations. The V3-V4 hypervariable region of the 16S rRNA gene was amplified using 338F (5'-ACTCCTACGGGAGGCAGCAG-3') and 806R (5'-GGACTACHVGGGTWTCTAAT-3') primers, respectively. PCR amplification was performed by a GeneAmp® PCR System 9700 (Applied Biosystems, USA) and the purified amplicons were sequenced with the MiSeq PE300 platform (Illumina, USA).

The raw data was initially quality-filtered by QIIME (v1.4.0-dev; QIIME development team)[29] and the operational units (OTUs) were clustered using UPARSE at 97% identity[30]. The taxonomy of each 16S rRNA gene sequence was analysed by RDP Classifier against the SILVA 16S rRNA database (SSU115, Max Planck Institute, Germany) with a 70% confidence threshold. The Chao1 (species richness), and the Shannon and Simpson (species diversity) indices were calculated using vegan packages in R (v3.4.4). Redundancy analysis (RDA) was performed in order to test the significant differences between samples and to identify the key variables that affect microbial communities.

2.6 Statistical analysis

SPSS 19.0 (IBM Corporation, Armonk, NY, USA) and Origin 8.5 (OriginLab, Northampton, MA, USA) were used to analyse and plot the data, respectively. A one-way ANOVA and post-hoc Duncan's multiple range test were used to compare ($p<0.05$) water quality parameters between different treatment systems at each sampling point.

3. Results and Discussion

3.1 Multifunctional geoengineering material characterisations

3.1.1 Porosity and composition

The BET surface area (52.86 m^2/g) and pore volume (0.22 cm^3/g) of the modified zeolite were significantly higher than those of natural zeolite, (38.07 m^2/g and 0.06 cm^3/g, respectively; Table 1). These changes were due to the calcination treatment under high temperature, which increased the pore size and volume of the zeolite[26]. The increased pore volume is expected to benefit the modified material, rendering it capable of carrying more O_2 nanobubbles and delivering them into the SWI during the application. The modification by $AlCl_3$ addition led to a significantly higher content of aluminium (Al) in the modified zeolite (23.37 wt%) than that in the natural zeolite (13.87 wt%). Al has been widely used as an additive in the preparation[31] of effective P adsorbents , because of its high affinity for phosphate and its interaction for enhancing P adsorption.

Table 1

The general characteristics of natural zeolite (Zeolite) and modified zeolite (M-Zeolite).

Materials	Fe (wt %)	Al (wt %)	Si (wt %)	Surface area (m^2/g)	Pore volume (cm^3/g)	Pore diameter (nm)
Natural zeolite	5.39	13.87	52.75	38.07	0.06	6.40
Modified zeolite	6.25	23.37	49.5	52.86	0.22	9.08

3.1.2 Morphology and characteristics

The morphology of natural zeolite appeared amorphous and coarse with many protrusions (Fig. 2a), however, the modified zeolite showed clear differences with many needle-shaped particles apparent (Fig. 2b). In the XRD pattern (Fig. 2c), the positions of

the main signals for natural and modified zeolites were similar, which indicated that the modification process did not destroy the rudimentary zeolite structure. However, some new signals appeared in the pattern for the modified zeolite at $2\theta = 12.86°$, $26.58°$, $31.76°$, which are characteristic for $AlCl_3$ (Jade software). In the FT-IR spectrum (Fig. 2d), broad band hydration signals, centred on 3447, 1638 and 1634 cm^{-1} are characteristic of the hydroxyl group[32], with the stretching and bending vibrations due to adsorbed water. The intensities of the structural OH bands, decreased in the spectrum obtained from the modified zeolite, which was an indication that physically absorbed water had been lost and that the structure had been partially destroyed, changes induced by calcination. The bands characteristic of Si-O bonds (1099, 1095 and 1091 cm^{-1}) appeared in both zeolites, indicated that the silicate minerals had been highly resistant to modification under high temperature[33]. Once again, the band at 793 cm^{-1}, corresponding to Al-O-Al stretching vibrations, only appeared in the modified zeolite. The aforementioned characteristics indicated the successful addition of Al into the modified zeolite, potentially increasing its P adsorption capability.
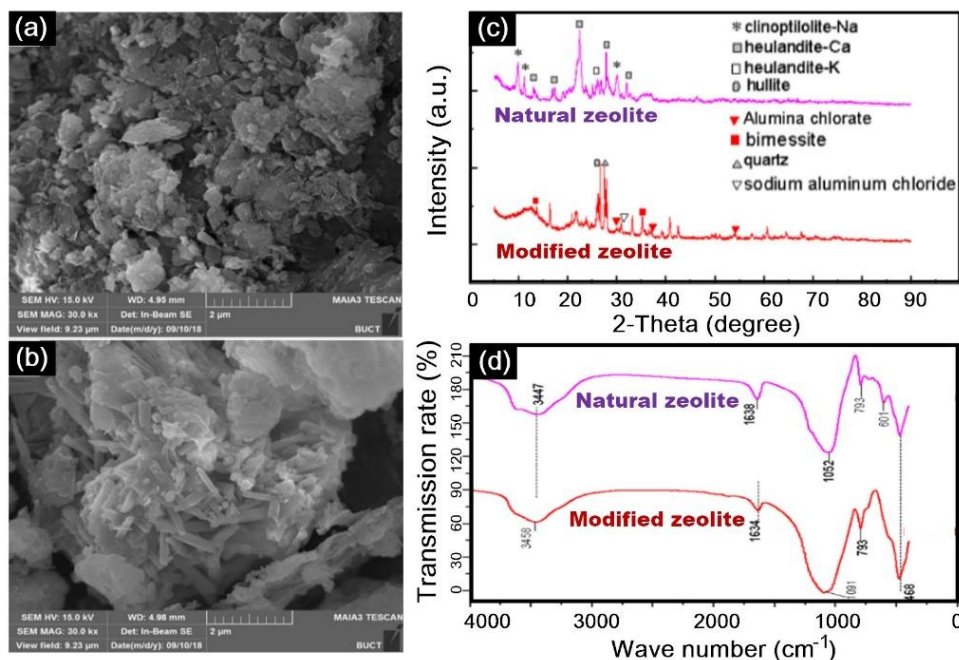

Fig. 2. Scanning electron microscope (SEM) images of natural (a) and modified (b) zeolites, and their characterisation by X-ray powder diffraction (XRD, c) and Fourier Transform infrared spectrum (FT-IR, d).

3.1.3 Adsorption isotherms and O_2 loading capacity

Phosphate (P) and ammonium (N) adsorption isotherms for both natural and modified zeolites exhibited L-shape curves (Fig. 3a and b), which all fitted the Langmuir model ($R^2 > 0.992$, Table S1). Significantly higher P adsorption capacity (Q_m 4.38 mg/g) was achieved by the modified zeolite compared with that of natural zeolite (Q_m 1.05 mg/g), which may be attributable to the addition of Al^{3+} (Fig. 2). The improved pore volume and BET surface area (Table 1) of modified zeolite may have led to the enhanced capability for N adsorption (Q_m 9.81 mg/g) compared with that of natural zeolite (Q_m 6.29 mg/g). The enhanced adsorption capacities of N and P will fix more nutrients and thus lead to less release of nutrients from the sediment to the overlying water during the capping treatment.

The O_2-TPD traces (Fig. 3c) clearly exhibited significantly higher desorption peaks for the modified zeolite than those of natural zeolite in the temperature ranges of 50-250°C and 300-600°C, respectively. Integration of the desorption traces indicated that the total peak area of O_2 desorbed from modified zeolites was around 20-fold higher than that from natural zeolites. Quantitative thermogravimetric (TG) analyses generally agreed with the relevant O_2-TPD data (Fig. 3d), where a smaller mass loss occurred at lower temperatures (<250°C) but considerable mass loss ensued for both materials when the temperature rose above 300°C. Notably, calcination and pre-drying treatments could theoretically minimize the content of the adhered water and crystalline components[34]. Thus, the O_2 desorbed at lower temperatures would be mainly that physically adsorbed by the material[35]. The O_2 mass loss at high temperatures may mainly exist as oxygen chemisorbed by the material. During the whole test, modified zeolite was demonstrated to carry 121 mg O_2/g, which is 2.6 times higher than that of natural zeolite (46 mg O_2 /g), based on the mass loss during O_2 desorption. The higher O_2 loading capacity was consistent with the increased surface area and pore volume possessed by modified zeolite (Table 1), which further suggests that oxygen carrying capacity is more likely linked to the existence of mesoporous voids in the capping material[36].
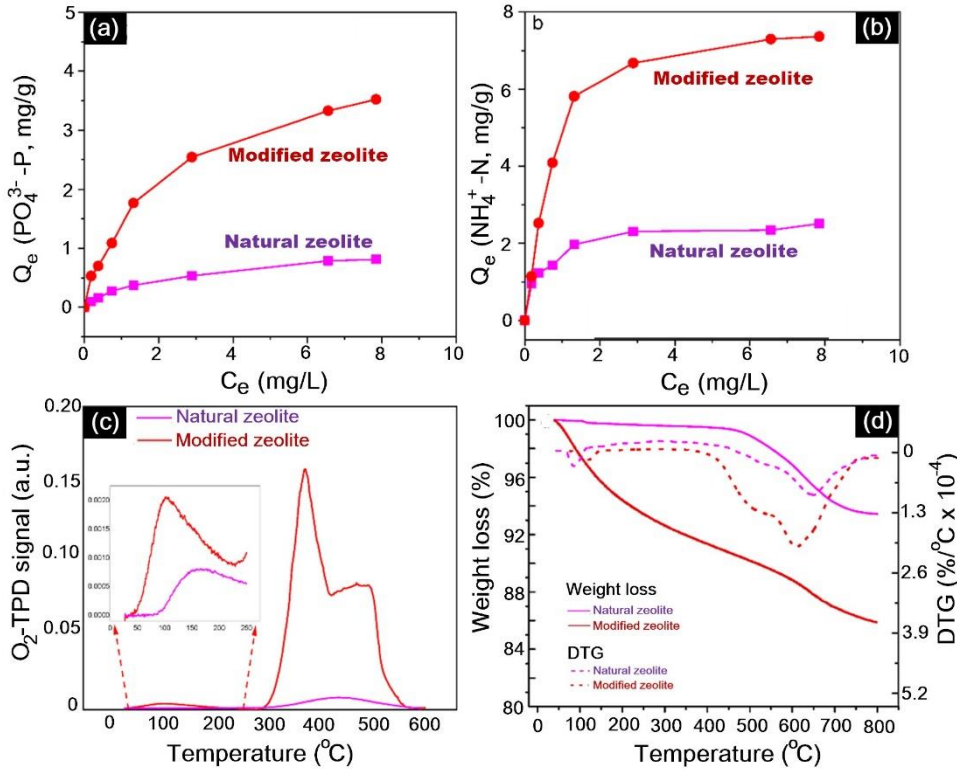
Fig. 3. Phosphate (a) and ammonium (b) adsorption isotherms of natural and modified zeolites. O_2-TPD patterns (c) and TG-DTG curves (d) from the O_2 adsorption capability test.

3.2 *In-situ experiment evaluation*

3.2.1 *DO and ORP dynamics at the sediment-water interfaces*

The *in-situ* experiment was conducted in a eutrophic shallow lake, which maintained constant low DO (~1.5 mg/L, Fig. 4a) and ORP (~-200 mV, Fig. 4b) levels of the overlying water in the control mesocosms throughout the experiment. After applying the capping material, the physical barrier thus formed above the sediment could stop release of anaerobic substances back to the water[14]. It could be the reason that the natural zeolite capping treatment managed to slightly increase DO to 2 mg/L and ORP levels to -100 mV. The modified zeolite, even without O_2 nanobubble loading, was observed to drive a clear increase in DO and ORP levels to 3.3 mg/L and -50 mV from day 9, respectively, which induced better hypoxia-combating conditions than did the natural zeolite but was still much less efficient than MFG. This effect may be due to the presence of more micropores in the modified zeolites (Table1), which may have carried more trace air due to exposure to the atmosphere after the capping operation[36]. This may have, in turn, activated more oxidised substances, such as iron oxide[23], thus resulting in a slightly

higher oxidising environment than that present in the natural zeolite and control groups.

In the mesocosms capped with the multifunctional geoengineering material, the DO of overlying waters rapidly increased from 1.5 to 6.2 mg/L, and ORP from -200 to 175 mV, in the first 5 days and then remained stable until the end of experiment. The successful reversal from hypoxia at the SWI to aerobic conditions was attributed to the synergistic functionalities of the formation of a physical barrier by the capping material and prolonged, sustainable, O_2 nanobubble delivery, which were in accord with previous studies[23, 24]. Under such interfacial O_2 nanobubble treatment, nano-scale (<200 nm) O_2 bubbles could be constantly released, forming an oxygen-locking layer at the SWI[22]. This mode of action is different from the traditional aeration methods of inducing large gas/oxygen bubbles. The O_2 nanobubbles possess unique characteristics of long lifetimes and high gas dissolvability[37], therefore supporting the reversal of the initial conditions of hypoxia to the final aerobic status.
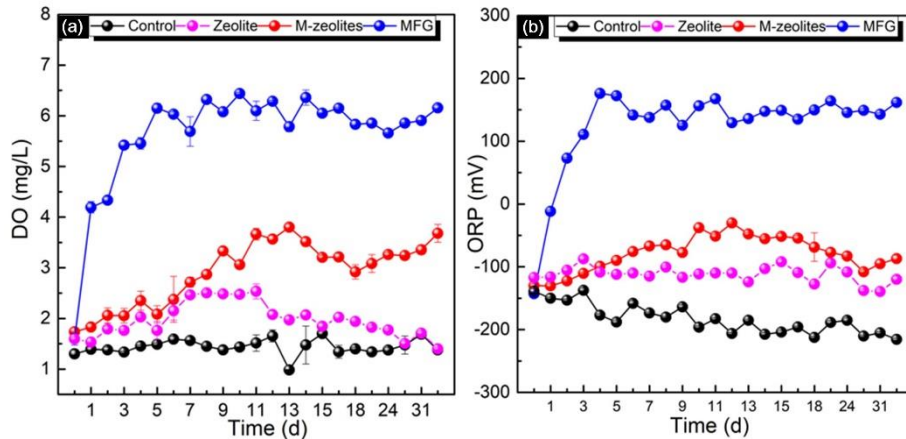

Fig. 4. Dynamics of DO (a) and ORP (b) at the SWI in different treated systems. Zeolite and M-zeolite represent natural and modified zeolites, respectively. MFG (multifunction geoengineering material) represents the O_2 nanobubble-loaded modified zeolite.

3.2.2 Nutrient dynamics and nutrient flux at SWI

Sediment hypoxia is a common phenomenon in eutrophic and/or highly polluted water bodies, where there is usually significant release of internal (*ie sediment-borne*) pollutants[17]. It is well known that release of both P and N from sediments can be significantly accelerated under hypoxic/anoxic conditions[18]. Thus, with reference to our mesocosm experiments, the continual lower DO/ORP levels in the control systems (Fig.

4) led to gradually increased concentrations of PO_4^{3-}-P and NH_4^+-N within overlying waters, which attained around 0.085 and 0.56 mg/L, respectively (Fig. 5a and b). The N and P concentrations in the control groups are clearly higher than the nutrient limitation to avoid the HABs and eutrophication occurrence in freshwaters[38]. Based on calculations, the fluxes of nutrients from sediment to overlying water showed positive values of 1.9-6.8 mg/m^2/d for P, and 4.8-19.7 mg/m^2/d for N (Fig. 5c and d) throughout the duration of the experiment. It is clear that further approaches may be required towards mitigation of the internal nutrient loadings.

With reference to control of the release of internal P, the concentrations of PO_4^{3-}-P in overlying water were significantly lower at the end of the experiment in the MFG treatment groups (~0.02 mg/L), followed by the modified (~0.06 mg/L) and natural (~0.075 mg/L) zeolite mesocosms (Fig. 5a). Only the MFG treatment group yielded a negative P flux (-1.69 to -0.34 mg/m^2/d) compared with the other groups (Fig. 5c). The enhanced performance of modified zeolite was attributable to the larger adsorption capacity for P than that observed from the natural zeolite (Fig. 3a), since the Al content in the modified zeolite particles (Fig. 2) could adsorb P through the formation of an insoluble phosphate (Al-PO$_4$), precipitated onto the mineral surface[39]. When extra O_2 was delivered at the SWI by MFG, in addition to the physicochemical adsorption of P by the modified zeolites, the O_2 could actively change the valence of any metals present, such as iron to facilitate formation of Fe-P[23]. This could explain the significant higher efficiency of MFG in reducing P concentrations in the overlying water, and the P influx observed across the SWI.

Regarding mitigation of the internal N loading, the dynamics of NH_4^+-N concentrations in the overlying waters were generally similar to those for P and follow the order MFG > modified zeolite ≥ natural zeolite > control systems (Fig. 5b). Although the modified zeolites possessed significantly higher NH_4^+-N adsorption capacities than did the natural zeolite during the batch experiment (Fig. 3b), however, both materials functioned similarly to reduce the NH_4^+-N concentration in overlying water (~0.4 mg/L at day 35) and flux (~3.65 mg/m^2/d) through the SWI. This may have been due to the

presence of co-existing, competitive, ions, such as Na^+, K^+, Ca^{2+}, and Mg^{2+}, that probably existed in the sediment, which acted to dramatically reduce NH_4^+-N adsorption during the application of the capping material[40]. The changed oxygen levels in MFG-treated mesocosms (Fig. 4) could affect N transformations mediated by bacterial activities at the SWI, particularly nitrification, denitrification and anammox reactions. The significant enhancement in DO concentrations at the SWI after adding MFG may have accelerated the nitrification process, converting NH_4^+-N to NO_3^--N[20]. This can be inferred from the fact that lower NH_4^+-N, whereas higher NO_3^--N and NO_2^--N, occurred in the mesocosms treated by MFG during the experiment (Fig. S1). As a result, application of MFG effectively improved the water quality through regulating the biogeochemical process to reduce NH_4^+-N level in the water.
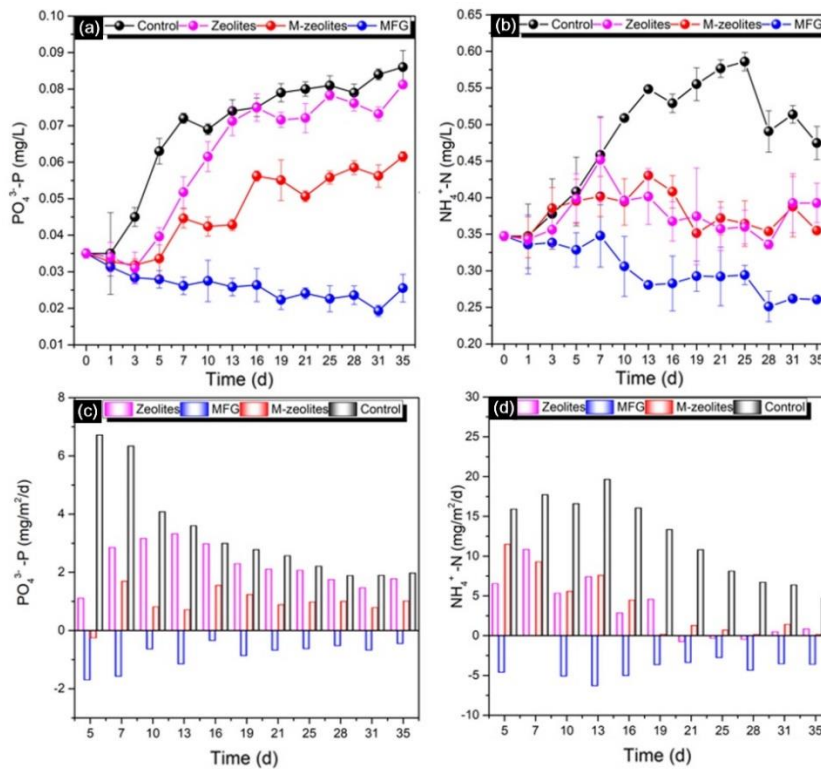

Fig. 5. Dynamics of PO_4^{3-}-P (a) and NH_4^+-N (b) in the overlaying water, and fluxes of PO_4^{3-}-P (c) and NH_4^+-N (d) across the SWI in each system. Zeolite and M-zeolite represent natural and modified zeolites, respectively. MFG (multifunction geoengineering material) represents the O_2 nanobubble-loaded modified zeolite.

3.2.3 Quantitative analysis of different functions for internal load control

Both capping treatment[14] and O_2 nanobubble technology[22] have been previously

demonstrated successfully for control of eutrophication. However, the respective contributions of capping treatment and hypoxia remediation are unclear during combating the internal nutrient release. In this study, the mass balance calculation according to the fluxes of P and N was conducted to quantify difference functions, i.e. capping treatment, modification to improve P&N adsorption, and O_2 delivery, on internal nutrient load control (Fig. 6). The highest released P and N amount from sediment were 2.93 (Fig. 6a1) and 11.42 mg (Fig. 6b1) respectively, throughout the 35-day experiment, occurring in the control mesocosms. After treatment by the natural zeolites, the amounts released decreased to 2.21 mg P and 2.90 mg N. The results indicated that, in isolation, the capping treatment utilising natural zeolites could reduce around 24.6% and 74.6% of the P and N release, respectively (Fig. 6a2 and b2). The internal loading of P in the system treated by the modified zeolites was 0.96 mg. After subtracting the contribution from the capping treatment alone, the modified zeolite could furnish a further reduction of 42.7% of the P release (Fig. 6a3). However, this material modification only contributed a further 0.4% reduction for control of the internal N loading. This agrees with the similar N concentration dynamics in the overlying waters (Fig. 5b), which have may been due to N adsorption under the presence of competitive ions in the sediment[40].

Both P and N fluxes were totally reversed in the MFG-treated groups (Fig. 5c and d) and the total masses fixed were 0.72 and 3.55 mg, respectively (Fig.6a4 and b4), which substantially changed the sediment from a nutrient source to a sink. In addition to zeolite capping and modification, the effect of the O_2 nanobubble oxidation contributed further reductions of 57.3% P and 56.1% N, compared with the control systems. This quantitative analysis demonstrated that the synthetically modified multifunctional geoengineering material could integrate all functionalities (i.e., physical capping, adsorption, and oxidation) and provided sustainable synergistic effects to mitigate the internal nutrient loadings.
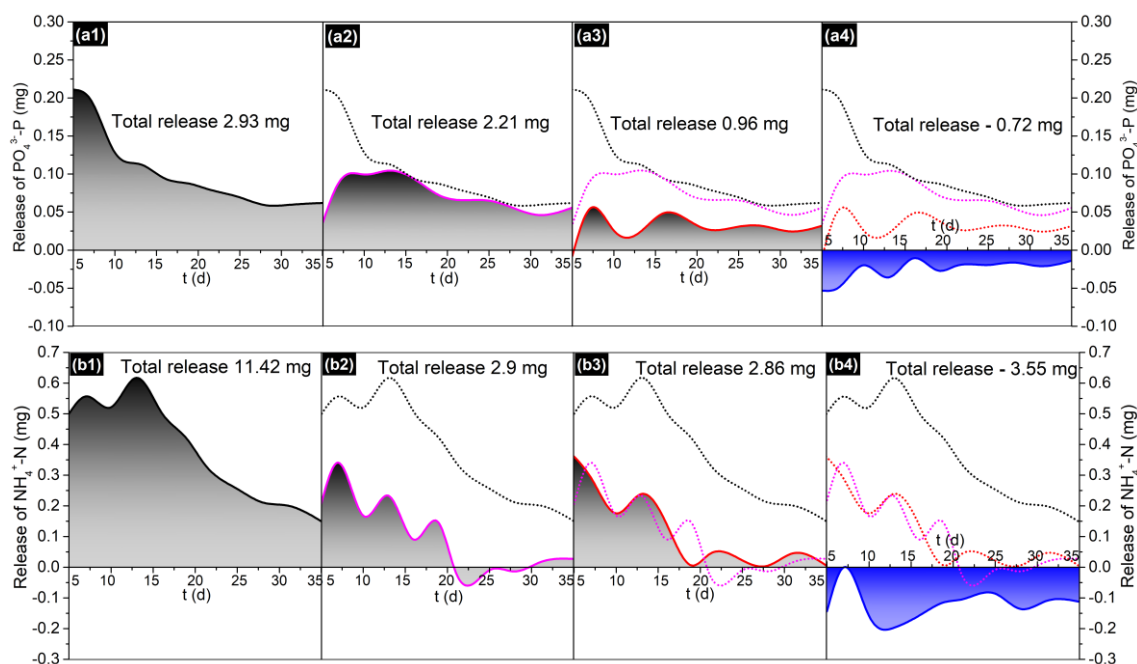
Fig. 6. Quantitative analysis of the treatment by natural zeolite (a2 and b2), modified zeolite (a3 and b3) and MFG (a4 and b4) for internal PO_4^{3-}-P (a) and NH_4^+-N (b) releases compared with the control systems (a1 and b1). The black, pink, red, and blue lines refer to internal nutrients （PO_4^{3-}-P (a) and NH_4^+-N(b)） releases in control systems, natural zeolite, modified zeolite, and MFG systems, respectively. MFG (multifunction geoengineering material) represents the O_2 nanobubble-loaded modified zeolite.

3.2.4 Alterations in microbial community composition

Sediment microbial community compositions in all four systems were analysed at the beginning and end of the experiment for comparison. After quality trimming, a total of 11,455 OTUs belonging to 60 phyla and 1,319 genera were extracted from 24 samples and the Good's coverage estimator of over 95% suggested that most of bacterial OTUs in each sample had been captured (Table S2). The highest microbial diversity (Shannon and Simpson index values) in the mesocosm after the MFG treatment indicated that O_2 nanobubbles could support a rich and diverse consortium for the biotransformation of nutrients, by establishing more complex oxygen gradients for bacterial survival, potentially resulting in the observed reductions in N and P release from the sediment.

The microbial communities showed high diversity at the phylum level with the major phyla being identified as *Proteobacteria, Chloroflexi, Actinobacteria,*

Acidobacteria, Bacteroidetes, Firmicutes, Nitrospirae, Latescibacteria, Patescibacteria and Spirochaetes (Fig. 7a). The in-situ samples for all systems showed certain variation, thus, the microbial community changes were specifically compared between each system before and after the treatment (Fig. S2). Significant improvements in the abundance of *Actinobacteria, Acidobacteria* and *Nitrospirae* were identified in the sediment after treatment by MFG. All three phyla were found to belong to typical ammonia oxidizing bacteria, which work in the nitrification process by transforming NH_4^+-N to NO_2^--N and then to NO_3^--N[41]. The MFG treatment groups in the RDA plot were clearly separated from the other systems (Fig. 7b), and DO was calculated to be the main driving factor ($p<0.05$) to differentiate the microbial community in MFG-treated mesocosms from the others (Table S3). It is understood that the nitrification reaction could be stimulated under aerobic conditions[20], which might have been caused by the delivery of O_2 nanobubbles and thus resulted in reduced NH_4^+-N release from the sediment back to the overlying water (Fig. 5b).
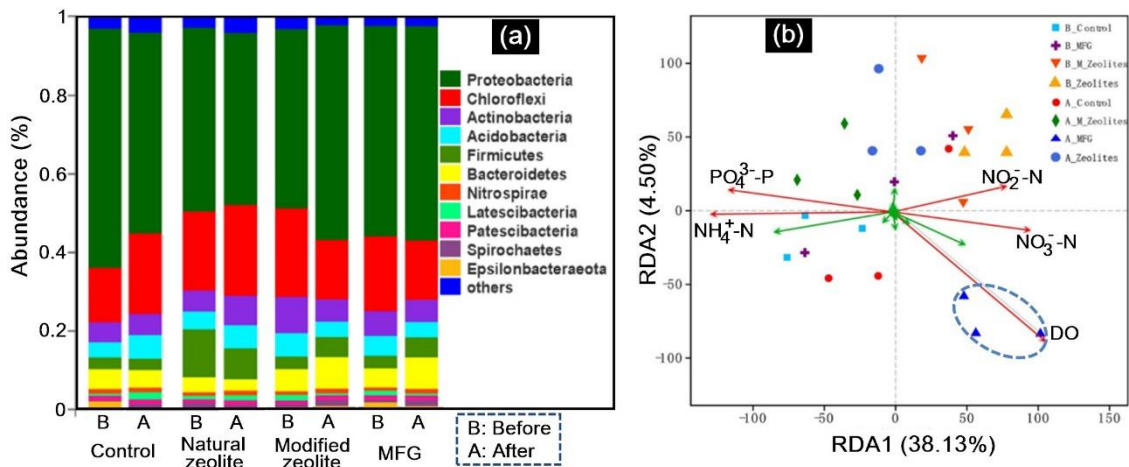

Fig. 7. Taxonomic classification of bacterial 16S rDNA gene reads of the sediment from the groups of control, natural zeolite, modified zeolite and MFG treatments at phylum level (a, relative abundances <1% not shown). Further redundancy analysis (RDA) plot (b) of relationships between environmental variables and bacterial community composition.

3.3 Insights for future environmental implication

Restoration of polluted waters can trigger the growth of submerged macrophytes, which play a crucial role in sustaining the cleared state[42]. However, this is difficult to

achieve in eutrophic or black, odorous, water bodies due to both constant internal nutrient release from sediment and to the persistence of anoxic conditions in the benthic zone, even after external nutrient loading has been successfully controlled[43]. Our findings in the present work highlight the promise of practical viability for the application of such multifunctional geoengineering material (MFG) as an effective approach for eutrophication control though the multiple functionalities of physical isolation, nutrient adsorption, and O_2 delivery.

In-situ capping with MFG is a potentially effective technology to stabilize sediments, minimizing both re-suspension and transport, remediate sediment hypoxia and reduce fluxes of both P and N into overlying waters. The functional "O_2-rich" layer can form at the SWI, which would not only inhibit nutrient release and enhance nutrient retention capacity in sediment, improve the hypoxic/anoxic environments, but also create favourable conditions for re-establishment of submerged vegetation. The improved conditions are expected to provide a window of opportunity for the germination and growth of submerged macrophytes[24]. Once the submerged vegetation is successfully established, it can continue to take up the excessive nutrients from sediment[44], effectively mitigating further eutrophication. Apart from efficiency of nutrient removal, this approach has the advantage of low cost and low energy consumption for O_2 delivery, based on the materials movement under gravity after the application. However, the long-term effects of the application of MFG in extensive lake systems need to be further investigated.

Acknowledgements

References

1.   Conley, D. J.; Paerl, H. W.; Howarth, R. W.; Boesch, D. F.; Seitzinger, S. P.; Havens, K. E.; Lancelot, C.; Likens, G. E., Controlling eutrophication: nitrogen and phosphorus. *Science* **2009,** *323*, (5917), 1014-1015.

2.   Yin, H.; Wang, J.; Zhang, R.; Tang, W., Performance of physical and chemical methods in the co-reduction of internal phosphorus and nitrogen loading from the sediment of a black odorous river. *Sci. Total Environ.* **2019,** *663*, 68-77.

3.   Paerl, H. W.; Otten, T. G.; Kudela, R., Mitigating the Expansion of Harmful Algal Blooms Across the Freshwater-to-Marine Continuum. *Environ. Sci. Technol.* **2018,** *52*, (10), 5519-5529.

4.   Abell, J. M.; Özkundakci, D.; Hamilton, D. P., Nitrogen and phosphorus limitation of phytoplankton growth in New Zealand lakes: implications for eutrophication control. *Ecosystems* **2010,** *13*, (7), 966-977.

5.   Horppila, J., Sediment nutrients, ecological status and restoration of lakes. *Water Res.* **2019,** *160*, 206-208.

6.   Qin, B.; Zhou, J.; Elser, J. J.; Gardner, W. S.; Deng, J.; Brookes, J. D., Water Depth Underpins the Relative Roles and Fates of Nitrogen and Phosphorus in Lakes. *Environ. Sci. Technol.* **2020,** *54*, (6), 3191-3198.

7.   Liu, C.; Chen, K.; Wang, Z.; Fan, C.; Gu, X.; Huang, W., Nitrogen exchange across the sediment-water interface after dredging: The influence of contaminated riverine suspended particulate matter. *Environ. Pollut.* **2017,** *229*, 879-886.

8.   Bierlein, K. A.; Rezvani, M.; Socolofsky, S. A.; Bryant, L. D.; Wüest, A.; Little, J. C., Increased sediment oxygen flux in lakes and reservoirs: The impact of hypolimnetic oxygenation. *Water Resour. Res.* **2017,** *53*, (6), 4876-4890.

9.   Jin, X.; Bi, L.; Lyu, T.; Chen, J.; Zhang, H.; Pan, G., Amphoteric starch-based bicomponent modified soil for mitigation of harmful algal blooms (HABs) with broad salinity tolerance: Flocculation, algal regrowth, and ecological safety. *Water Res.* **2019,** *165*, 115005.

10.   Li, X. D.; Zhang, Z. Y.; Xie, Q.; Yang, R. J.; Guan, T.; Wu, D. Y., Immobilization and Release Behavior of Phosphorus on Phoslock-Inactivated Sediment under Conditions Simulating the Photic Zone in Eutrophic Shallow Lakes. *Environ. Sci. Technol.* **2019,** *53*, (21), 12449-12457.

11. Huser, B. J.; Futter, M.; Lee, J. T.; Perniel, M., In-lake measures for phosphorus control: The most feasible and cost-effective solution for long-term management of water quality in urban lakes. *Water Res.* **2016,** *97*, 142-152.

12. Lürling, M.; Mackay, E.; Reitzel, K.; Spears, B. M., Editorial – A critical perspective on geo-engineering for eutrophication management in lakes. *Water Res.* **2016,** *97*, 1-10.

13. Pan, M.; Lyu, T.; Zhang, M.; Zhang, H.; Bi, L.; Wang, L.; Chen, J.; Yao, C.; Ali, J.; Best, S., Synergistic Recapturing of External and Internal Phosphorus for In Situ Eutrophication Mitigation. *Water* **2020,** *12*, (1), 2.

14. Gibbs, M. M.; Hickey, C. W., Flocculants and Sediment Capping for Phosphorus Management. In *Lake Restoration Handbook*, Springer: 2018; pp 207-265.

15. Silva, J. M. R.; Morais, E. K. L.; Silveira, J. B.; Oliveira, M. H. R.; Coriolano, A. C. F.; Fernandes, V. J.; Araujo, A. S., Improved thermogravimetric system for processing of oil sludge using HY zeolite catalyst. *J. Therm. Anal. Calorim.* **2019,** *136*, (4), 1861-1868.

16. Fang, L.; Liu, R.; Li, J.; Xu, C.; Huang, L.-Z.; Wang, D., Magnetite/Lanthanum hydroxide for phosphate sequestration and recovery from lake and the attenuation effects of sediment particles. *Water Res.* **2018,** *130*, 243-254.

17. Funkey, C. P.; Conley, D. J.; Reuss, N. S.; Humborg, C.; Jilbert, T.; Slomp, C. P., Hypoxia Sustains Cyanobacteria Blooms in the Baltic Sea. *Environ. Sci. Technol.* **2014,** *48*, (5), 2598-2602.

18. Testa, J. M.; Kemp, W. M., Hypoxia-induced shifts in nitrogen and phosphorus cycling in Chesapeake Bay. *Limnol. Oceanogr.* **2012,** *57*, (3), 835-850.

19. Chen, M.; Ding, S.; Wu, Y.; Fan, X.; Jin, Z.; Tsang, D. C.; Wang, Y.; Zhang, C., Phosphorus mobilization in lake sediments: experimental evidence of strong control by iron and negligible influences of manganese redox reactions. *Environ. Pollut.* **2019,** *246*, 472-481.

20. Lyu, T.; He, K. L.; Dong, R. J.; Wu, S. B., The intensified constructed wetlands are promising for treatment of ammonia stripped effluent: Nitrogen transformations and removal pathways. *Environ. Pollut.* **2018,** *236*, 273-282.

21. Conley, D. J.; Bonsdorff, E.; Carstensen, J.; Destouni, G.; Gustafsson, B. G.; Hansson, L. A.; Rabalais, N. N.; Voss, M.; Zillen, L., Tackling Hypoxia in the Baltic Sea: Is Engineering a Solution? *Environ. Sci. Technol.* **2009,** *43*, (10), 3407-3411.

22.	Zhang, H.; Lyu, T.; Bi, L.; Tempero, G.; Hamilton, D. P.; Pan, G., Combating hypoxia/anoxia at sediment-water interfaces: A preliminary study of oxygen nanobubble modified clay materials. *Sci. Total Environ.* **2018,** *637–638*, 550-560.

23.	Yu, P.; Wang, J.; Chen, J.; Guo, J.; Yang, H.; Chen, Q., Successful control of phosphorus release from sediments using oxygen nano-bubble-modified minerals. *Sci. Total Environ.* **2019**.

24.	Zhang, H.; Chen, J.; Han, M.; An, W.; Yu, J., Anoxia remediation and internal loading modulation in eutrophic lakes using geoengineering method based on oxygen nanobubbles. *Sci. Total Environ.* **2020,** *714*, 136766.

25.	Shi, W.; Pan, G.; Chen, Q.; Song, L.; Zhu, L.; Ji, X., Hypoxia Remediation and Methane Emission Manipulation Using Surface Oxygen Nanobubbles. *Environ. Sci. Technol.* **2018,** *52*, (15), 8712-8717.

26.	Liang, Z.; Ni, J. R., Improving the ammonium ion uptake onto natural zeolite by using an integrated modification process. *J. Hazard. Mater.* **2009,** *166*, (1), 52-60.

27.	Zhang, L.; Wang, S.; Jiao, L.; Zhao, H.; Zhang, Y.; Li, Y., Physiological response of a submerged plant (Myriophyllum spicatum) to different NH_4Cl concentrations in sediments. *Ecol.Eng. 2***013,** *58*, 91-98.

28.	APHA, Standard methods for the examination of water and wastewater. *American Public Health Association (APHA): Washington, DC, USA* **2005**.

29.	Caporaso, J. G.; Kuczynski, J.; Stombaugh, J.; Bittinger, K.; Bushman, F. D.; Costello, E. K.; Fierer, N.; Pena, A. G.; Goodrich, J. K.; Gordon, J. I., QIIME allows analysis of high-throughput community sequencing data. *Nature methods* **2010,** *7*, (5), 335.

30.	Bai, S.; Lyu, T.; Ding, Y.; Li, Z.; Wang, D.; You, S.; Xie, Q., Campus sewage treatment in multilayer horizontal subsurface flow constructed wetlands: Nitrogen removal and microbial community distribution. *CLEAN–Soil, Air, Water* **2017,** *45*, (11), 1700254.

31.	Huser, B. J.; Egemose, S.; Harper, H.; Hupfer, M.; Jensen, H.; Pilgrim, K. M.; Reitzel, K.; Rydin, E.; Futter, M., Longevity and effectiveness of aluminum addition to reduce sediment phosphorus release and restore lake water quality. *Water Res.* **2016,** *97*, 122-132.

32.	Kizito, S.; Luo, H. Z.; Wu, S. B.; Ajmal, Z.; Lv, T.; Dong, R. J., Phosphate recovery from liquid fraction of anaerobic digestate using four slow pyrolyzed biochars: Dynamics of adsorption, desorption and regeneration. *J. Environ. Manag.* **2017,** *201*, 260-267.

33.	Yin, H. B.; Kong, M.; Fan, C. X., Batch investigations on P immobilization from wastewaters and sediment using natural calcium rich sepiolite as a reactive material. *Water Res.* **2013,** *47*, (13), 4247-4258.

34.   Cantú, M.; López-Salinas, E.; Valente, J. S., SOx removal by calcined MgAIFe hydrotalcite-like materials: Effect of the chemical composition and the cerium incorporation method. *Environ. Sci. Technol.* **2005,** *39*, (24), 9715-9720.

35.   Kontogiannidou, E.; Karavasili, C.; Kouskoura, M. G.; Filippousi, M.; Van Tendeloo, G.; Andreadis, I. I.; Eleftheriadis, G. K.; Kontopoulou, I.; Markopoulou, C. K.; Bouropoulos, N., In vitro and ex vivo assessment of microporous Faujasite zeolite (NaX-FAU) as a carrier for the oral delivery of danazol. *J DRUG DELIV SCI TEC* **2019,** *51*, 177-184.

36.   Liu, M.; Ran, Y.; Peng, X.; Zhu, Z.; Liang, J.; Ai, H.; Li, H.; He, Q., Sustainable modulation of anaerobic malodorous black water: The interactive effect of oxygen-loaded porous material and submerged macrophyte. *Water Res.* **2019,** *160*, 70-80.

37.   Lyu, T.; Wu, S.; Mortimer, R. J. G.; Pan, G., Nanobubble Technology in Environmental Engineering: Revolutionization Potential and Challenges. *Environ. Sci. Technol.* **2019**.

38.   Tong, Y.; Xu, X.; Zhang, S.; Shi, L.; Zhang, X.; Wang, M.; Qi, M.; Chen, C.; Wen, Y.; Zhao, Y.; Zhang, W.; Lv, X., Establishment of season-specific nutrient thresholds and analyses of the effects of nutrient management in eutrophic lakes through statistical machine learning. *J HYDROL* **2019**, 124079.

39.   Guaya, D.; Valderrama, C.; Farran, A.; Armijos, C.; Cortina, J. L., Simultaneous phosphate and ammonium removal from aqueous solution by a hydrated aluminum oxide modified natural zeolite. *Chem. Eng. J.* **2015,** *271*, 204-213.

40.   Kontogiannidou, E.; Karavasili, C.; Kouskoura, M. G.; Filippousi, M.; Van Tendeloo, G.; Andreadis, I. I.; Eleftheriadis, G. K.; Kontopoulou, I.; Markopoulou, C. K.; Bouropoulos, N.; Fatouros, D. G., In vitro and ex vivo assessment of microporous Faujasite zeolite (NaX-FAU) as a carrier for the oral delivery of danazol. *J DRUG DELIV SCI TEC* **2019,** *51*, 177-184.

41.   Wagner, M.; Loy, A.; Nogueira, R.; Purkhold, U.; Lee, N.; Daims, H., Microbial community composition and function in wastewater treatment plants. *Anton Leeuw Int J G* **2002,** *81*, (1-4), 665-680.

42.   Spears, B. M.; Mackay, E. B.; Yasseri, S.; Gunn, L. D. M.; Waters, K. E.; Andrews, C.; Cole, S.; De Ville, M.; Kelly, A.; Meis, S.; Moore, A. L.; Nurnberg, G. K.; van Oosterhout, F.; Pitt, J. A.; Madgwick, G.; Woods, H. J.; Lurling, M., A meta-analysis of water quality and aquatic macrophyte responses in 18 lakes treated with lanthanum modified bentonite (Phoslock (R)). *Water Res.* **2016,** *97*, 111-121.

43.   Lyu, T.; Song, L.; Chen, Q.; Pan, G., Lake and River Restoration: Method, Evaluation and Management. *Water* **2020,** *12*, (4), 977.

44. Zhang, H.; Shang, Y.; lyu, T.; Chen, J.; Pan, G., Switching Harmful Algal Blooms to Submerged Macrophytes in Shallow Waters Using Geo-engineering Methods: Evidence from a 15N Tracing Study. *Environ. Sci. Technol.* **2018,** *52*, (20), 11778-11785.